

FLEXURAL VIBRATIONS OF FREE CIRCULAR PLATES ELASTICALLY CONSTRAINED ALONG PARTS OF THE EDGE

YOSHIHIRO NARITA† and ARTHUR W. LEISSA

Department of Engineering Mechanics, Ohio State University, Columbus, OH 43210, U.S.A.

(Received 11 February 1980)

Abstract—The present paper deals with the free transverse vibration of a circular plate elastically constrained along parts of its edge and free on the remainder. The elastic constraints considered permit both translational and/or rotational springs of space-varying stiffness. The analytical method utilized depends upon expanding both piecewise constant spring stiffnesses in the present problem into their Fourier components around the circumference of the plate. Numerical results are presented which demonstrate the effectiveness of the method and show interesting variations of the frequencies and nodal patterns over a range of constraint parameters. As special cases, numerical results are also given for the problem of the plate which is partially free and partially simply supported, as well as for the clamped-free boundary.

NOTATION

A_n, A_n^*	coefficient of regular Bessel function
C_n, C_n^*	coefficient of modified Bessel function
a	radius of a circular plate
D	flexural rigidity of a plate, $D = Eh^3/12(1 - \nu^2)$
E	Young's modulus
h	plate thickness
J_n	regular Bessel function of order n
I_n	modified Bessel function of order n
K_n, K_n^*	stiffnesses of distributed translational and rotational springs, respectively
$\bar{K}_n^{(t)}, \bar{K}_n^{(r)}$	nondimensional stiffnesses of i th translational and rotational springs, respectively
K_m, K_m^*, L_m, L_m^*	Fourier coefficients of spring stiffnesses
$\bar{K}_m, \bar{K}_m^*, \bar{L}_m, \bar{L}_m^*$	nondimensionalized Fourier coefficients of spring stiffnesses
k	$= \omega^{1/2}(\rho D)^{1/4}$
M_r	radial bending moment (moment/unit length)
n	index identifying circumferential Fourier components
V_r	edge reaction (force/unit length)
r	radial coordinate
s	number of interior nodal circles
W	transverse deflection
W_n	deflection function of the n th Fourier component
θ	circumferential coordinate
α	half-angle of the spring constraint
λ	nondimensional frequency parameter ($= \omega a^2 \sqrt{\rho D}$)
ν	Poisson's ratio
ρ	mass density (mass/unit area)
ω	circular frequency of free vibration
∇^2	Laplacian differential operator
∇^4	biharmonic differential operator ($= \nabla^2 \nabla^2$).

1. INTRODUCTION

The free vibration of plates has been a subject of considerable study, for reasons of both practical and academic interest and numerous publications have resulted. Various summaries of the available literature [1, 2] indicate that at least 1000 references exist which deal with such problems.

For a solid circular plate, the number of combinations of boundary conditions is only three, compared with the twenty-one distinct combinations which exist for a rectangular plate [3], as long as uniform, classical conditions of free, simply supported and clamped boundaries are considered. Numerous references for such problems can be found in the literature [1]. These boundary conditions are also obtained from the case of an elastically constrained boundary by taking two (translational and rotational) elastic constraints to be zero and/or infinity. Several

†Rotary Foundation Fellow, on leave from Hokkaido University, Sapporo 060, Japan.

references can be found in the literature which deal with the vibration problem of a circular plate having elastic springs distributed uniformly around its periphery [4-8].

However, difficulty in obtaining analytical solutions arises when non-uniform edge conditions are taken into consideration. For this reason, only a limited number of numerical results have been obtained concerning circular plates with non-uniform edges [9-16]. The first known solutions dealing with mixed boundary conditions involving elastic constraints is [17]. In that paper, the free vibrations of simply supported circular plates having partial rotational elastic constraints were analyzed by an extension of the method shown in [18]. The present work employs the same method under more general boundary conditions, namely a circular plate elastically constrained by partial translational and rotational springs, both along various portions of the edge. Frequency parameters and nodal patterns of circular plates having edges partly free and partly elastically constrained are presented and their variations over a range of parameters are discussed.

2. ANALYSIS

The free transverse vibration of a thin, homogeneous plate is governed by the differential equation

$$D\nabla^4 W - \rho\omega^2 W = 0 \quad (1)$$

where, in polar coordinates, $W = W(r, \theta)$. An exact solution to eqn (1) for a solid circular plate is given by

$$W(r, \theta) = \sum_{n=0}^{\infty} W_n(kr) \cos n\theta + \sum_{n=1}^{\infty} W_n^*(kr) \sin n\theta \quad (2)$$

where

$$W_n(kr) = A_n J_n(kr) + C_n I_n(kr) \quad (3a)$$

$$W_n^*(kr) = A_n^* J_n(kr) + C_n^* I_n(kr). \quad (3b)$$

Consider a free circular plate elastically constrained along parts of the edge as shown in Fig. 1. Some translational and rotational springs having stiffnesses $K_w^{(i)}$ and $K_\psi^{(i)}$, respectively, are attached to typical portions of the edge. Hence, the following boundary conditions are required

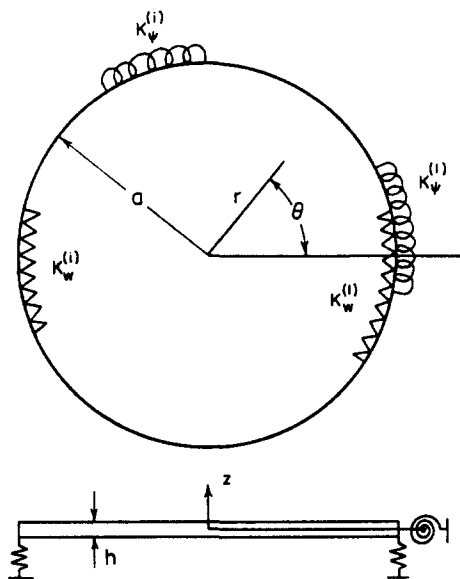


Fig. 1. Circular plate constrained by translational and rotational springs.

along constrained parts of the edge

$$V_r(a, \theta) = -K_w^{(i)} W(a, \theta) \quad (4a)$$

$$M_r(a, \theta) = K_\psi^{(i)} \frac{\partial W}{\partial r}(a, \theta) \quad (4b)$$

where the edge reaction and bending moment are related to the deflection by

$$V_r(r, \theta) = -D \left[\frac{\partial}{\partial r} (\nabla^2 W) + \frac{1-\nu}{r} \frac{\partial}{\partial r} \left(\frac{1}{r} \frac{\partial^2 W}{\partial \theta^2} \right) \right] \quad (5a)$$

$$M_r(r, \theta) = -D \left[\frac{\partial^2 W}{\partial r^2} + \nu \left(\frac{1}{r} \frac{\partial W}{\partial r} + \frac{1}{r^2} \frac{\partial^2 W}{\partial \theta^2} \right) \right]. \quad (5b)$$

Because the stiffnesses K_w , K_ψ of the entire spring system are assumed to vary along the edge, it is reasonable to expand them into Fourier series:

$$K_w(\theta) = \sum_{m=0}^{\infty} K_m \cos m\theta + \sum_{m=1}^{\infty} K_m^* \sin m\theta \quad (6a)$$

$$K_\psi(\theta) = \sum_{m=0}^{\infty} L_m \cos m\theta + \sum_{m=1}^{\infty} L_m^* \sin m\theta \quad (6b)$$

where K_m , K_m^* , L_m and L_m^* are the Fourier coefficients determined in the usual manner. Substitution of eqns (2), (5) and (6) into (4) yields

$$\begin{aligned} & \sum_{n=0}^{\infty} \{ \lambda^3 W_n''' + \lambda^2 W_n'' - \lambda [1 + n^2(2-\nu)] W_n' + n^2(3-\nu) W_n \} \cos n\theta \\ & + \sum_{n=1}^{\infty} \{ \lambda^3 W_n''' + \lambda^2 W_n'' - \lambda [1 + n^2(2-\nu)] W_n' + n^2(3-\nu) W_n^* \} \sin n\theta \\ & = f_1(\theta) + f_2(\theta) + f_3(\theta) + f_4(\theta) \end{aligned} \quad (7a)$$

$$\begin{aligned} & \sum_{n=0}^{\infty} \{ \lambda^2 W_n'' + \nu \lambda W_n' - \nu n W_n \} \cos n\theta + \sum_{n=1}^{\infty} \{ \lambda^2 W_n'' + \nu \lambda W_n' - \nu n W_n^* \} \sin n\theta \\ & = -\lambda [g_1(\theta) + g_2(\theta) + g_3(\theta) + g_4(\theta)] \end{aligned} \quad (7b)$$

where

$$\begin{aligned} f_1(\theta) &= \sum_{m=0}^{\infty} \bar{K}_m \cos m\theta \sum_{n=0}^{\infty} W_n \cos n\theta, \quad f_2(\theta) = \sum_{m=0}^{\infty} \bar{K}_m \cos m\theta \sum_{n=1}^{\infty} W_n^* \sin n\theta \\ f_3(\theta) &= \sum_{m=1}^{\infty} \bar{K}_m^* \sin m\theta \sum_{n=0}^{\infty} W_n \cos n\theta, \quad f_4(\theta) = \sum_{m=1}^{\infty} \bar{K}_m^* \sin m\theta \sum_{n=1}^{\infty} W_n^* \sin n\theta \\ g_1(\theta) &= \sum_{m=0}^{\infty} \bar{L}_m \cos m\theta \sum_{n=0}^{\infty} W_n' \cos n\theta, \quad g_2(\theta) = \sum_{m=0}^{\infty} \bar{L}_m \cos m\theta \sum_{n=1}^{\infty} W_n' \sin n\theta \\ g_3(\theta) &= \sum_{m=1}^{\infty} \bar{L}_m^* \sin m\theta \sum_{n=0}^{\infty} W_n' \cos n\theta, \quad g_4(\theta) = \sum_{m=1}^{\infty} \bar{L}_m^* \sin m\theta \sum_{n=1}^{\infty} W_n' \sin n\theta \end{aligned} \quad (8)$$

and where $\bar{K}_m, \dots, \bar{L}_m^*$ are nondimensional spring stiffness parameters defined by

$$\bar{K}_m = K_m a^3 / D, \quad \bar{K}_m^* = K_m^* a^3 / D, \quad \bar{L}_m = L_m a / D, \quad \bar{L}_m^* = L_m^* a / D \quad (9)$$

and the primes denote derivatives with respect to kr .

Suppose that the spring system has an axis of symmetry at $\theta = 0$. In this case, vibration modes reflect this symmetry and are separated into symmetric and anti-symmetric modes with respect to the axis. Then, we obtain

$$\{\lambda^3 W_n'''' + \lambda^2 W_n'' - \lambda[1 + n^2(2 - \nu)]W_n' + n^2(3 - \nu)W_n\} \begin{pmatrix} \cos n\theta \\ \sin n\theta \end{pmatrix} = \begin{pmatrix} f_1(\theta) \\ f_2(\theta) \end{pmatrix} \quad (10a)$$

$$\{\lambda^2 W_n'' + \nu\lambda W_n' - \nu n^2 W_n\} \begin{pmatrix} \cos n\theta \\ \sin n\theta \end{pmatrix} = -\lambda \begin{pmatrix} g_1(\theta) \\ g_2(\theta) \end{pmatrix} \quad (10b)$$

and $f_3(\theta) = f_4(\theta) = g_3(\theta) = g_4(\theta) = 0$. The functions $f_1(\theta), f_2(\theta), \dots$ can be rewritten as

$$f_1(\theta) = \begin{cases} K_0 W_0 + \frac{1}{2} \sum_{i=0}^{\infty} \bar{K}_i W_i & (n = 0) \\ \sum_{n=1}^{\infty} \left\{ \bar{K}_0 W_n + \frac{1}{2} \left[\bar{K}_n W_0 + \sum_{i=1}^{\infty} \bar{K}_i (W_{n+i} + W_{|n-i|}) \right] \right\} \cos n\theta \end{cases} \quad (11a)$$

$$f_2(\theta) = \sum_{n=1}^{\infty} \left\{ \bar{K}_0 W_n + \frac{1}{2} \left[\bar{K}_n W_0 + \sum_{i=1}^{\infty} \bar{K}_i (W_{n+i} \pm W_{|n-i|}) \right] \right\} \sin n\theta$$

$$\left(\pm : \begin{array}{l} n > i \\ n \leq i \end{array} \right) \quad (11b)$$

$$g_1(\theta) = \begin{cases} \bar{L}_0 W_0' + \frac{1}{2} \sum_{i=1}^{\infty} \bar{L}_i W_i' & (n = 0) \\ \sum_{n=1}^{\infty} \left\{ \bar{L}_0 W_n' + \frac{1}{2} \left[\bar{L}_n W_0' + \sum_{i=1}^{\infty} \bar{L}_i (W_{n+i}' + W_{|n-i|}') \right] \right\} \cos n\theta \end{cases} \quad (11c)$$

$$g_2(\theta) = \sum_{n=1}^{\infty} \left\{ \bar{L}_0 W_n' + \frac{1}{2} \left[\bar{L}_n W_0' + \sum_{i=1}^{\infty} \bar{L}_i (W_{n+i}' \pm W_{|n-i|}') \right] \right\} \sin n\theta$$

$$\left(\pm : \begin{array}{l} n > i \\ n \leq i \end{array} \right) \quad (11d)$$

by use of the trigonometric identities such as

$$\cos m\theta \sin n\theta = \frac{1}{2} [\cos(m-n)\theta + \sin(m-n)\theta]. \quad (12)$$

Derivatives of Bessel functions with respect to kr are evaluated by the formulas

$$J_n'(\lambda) = \frac{n}{\lambda} J_n(\lambda) - J_{n+1}(\lambda) \quad (13a)$$

$$I_n'(\lambda) = \frac{n}{\lambda} I_n(\lambda) + I_{n+1}(\lambda). \quad (13b)$$

The derivatives of higher order are also obtained by the repetition of these formulas and it is advantageous to reduce the order of the Bessel functions by making use of the well-known recursion formulas. Equating the coefficients of $\cos n\theta$ and $\sin n\theta$ in eqns (10) and substituting eqns (3) yields the following frequency equations in matrix form.

(1) Symmetric mode

$$\begin{bmatrix} E_{00} & E_{01} & E_{02} & \cdots \\ E_{10} & E_{11} & E_{12} & \cdots \\ E_{20} & E_{21} & E_{22} & \cdots \\ \vdots & \vdots & \vdots & \ddots \end{bmatrix} \begin{bmatrix} C_0 \\ C_1 \\ C_2 \\ \vdots \end{bmatrix} = 0 \tag{14}$$

where

$$E_{00} \equiv 2 \begin{bmatrix} -\rho(0) - \bar{\rho}_0(0) \\ \frac{1}{\lambda} q(0) \quad \frac{1}{\lambda} \bar{q}_0(0) \end{bmatrix}, E_{0j} \equiv \begin{bmatrix} \bar{K}_j J_j & \bar{K}_j I_j \\ \bar{L}_j J'_j & \bar{L}_j I'_j \end{bmatrix} \tag{15a, b}$$

(j = 1, 2, ...)

$$E_{jj} \equiv \begin{bmatrix} -2\rho(j) + \bar{K}_2 J_j & -2\bar{\rho}(j) + \bar{K}_2 I_j \\ \frac{2}{\lambda} q(j) + \bar{L}_2 J'_j & \frac{2}{\lambda} \bar{q}(j) + \bar{L}_2 I'_j \end{bmatrix} \tag{15c}$$

$$E_{i, j} \equiv \begin{bmatrix} (\bar{K}_{|i-j|} + \bar{K}_{i+j}) J_j & (\bar{K}_{|i-j|} + \bar{K}_{i+j}) I_j \\ (\bar{L}_{|i-j|} + \bar{L}_{i+j}) J'_j & (\bar{L}_{|i-j|} + \bar{L}_{i+j}) I'_j \end{bmatrix} \quad \begin{matrix} (i = 1, 2, \dots) \\ (j = 1, 2, \dots) \end{matrix} \tag{15d}$$

$$C_i \equiv \begin{bmatrix} A_i \\ C_i \end{bmatrix} \quad (i = 0, 1, 2, \dots) \tag{15e}$$

and

$$\begin{aligned} \rho(n) &= [n^2(1-n)(1-\nu) - n\lambda^2 - \bar{K}_0] J_n + \lambda[n^2(1-\nu) + \lambda^2] J_{n+1} \\ \bar{\rho}(n) &= [n^2(1-n)(1-\nu) - n\lambda^2 - \bar{K}_0] I_n - \lambda[n^2(1-\nu) - \lambda^2] I_{n+1} \\ q(n) &= [n(1-n)(1-\nu) - \lambda^2 + n\bar{L}_0] J_n + \lambda(1-\nu - \bar{L}_0) J_{n+1} \\ \bar{q}(n) &= [n(1-n)(1-\nu) + \lambda^2 + n\bar{L}_0] I_n - \lambda(1-\nu - \bar{L}_0) I_{n+1}. \end{aligned} \tag{16}$$

(2) Anti-symmetric mode

$$\begin{bmatrix} E_{11} & E_{12} & E_{13} & \cdots \\ E_{21} & E_{22} & E_{23} & \cdots \\ E_{31} & E_{32} & E_{33} & \cdots \\ \vdots & \vdots & \vdots & \ddots \end{bmatrix} \begin{bmatrix} C_1 \\ C_2 \\ C_3 \\ \vdots \end{bmatrix} \tag{17}$$

where

$$E_{jj} = \begin{bmatrix} -2\rho(j) - \bar{K}_2 J_j & -2\bar{\rho}(j) - \bar{K}_2 I_j \\ \frac{2}{\lambda} q(j) - \bar{L}_2 J'_j & \frac{2}{\lambda} \bar{q}(j) - \bar{L}_2 I'_j \end{bmatrix} \quad (j = 1, 2, \dots)$$

$$E_{i, j} = \begin{bmatrix} (\bar{K}_{|i-j|} - \bar{K}_{i+j}) J_j & (\bar{K}_{|i-j|} - \bar{K}_{i+j}) I_j \\ (\bar{L}_{|i-j|} - \bar{L}_{i+j}) J'_j & (\bar{L}_{|i-j|} - \bar{L}_{i+j}) I'_j \end{bmatrix} \quad (i, j = 1, 2, \dots). \tag{18}$$

The natural frequencies of the plate are obtained by calculating the eigenvalues of the determinants of the coefficient matrices of eqns (14) and (17) and mode shapes are determined by eqn (2) after solving eqns (14) and (17) in terms of amplitude ratio C_i/A_0 or C_i/A_1 .

3. NUMERICAL EXAMPLES

When a circular plate is uniformly constrained along the entire edge, the frequency equation is considerably simplified and the exact frequency parameters can be readily obtained. For example, frequency parameters (λ) for a circular plate uniformly constrained by a translational spring are presented in Table 1. The mode shapes are identified by (n, s) , where n and s are the number of internal nodal diameters and circles, respectively. For a completely free plate ($K_w = 0$), the lowest and second frequency vanish and the plate physically shows rigid body motions of translation and rotation, respectively. As the nondimensional stiffness ($K_w a^3/D$) is increased, the frequency parameters become higher and approach those for a simply supported plate when a stiffness $K_w a^3/D = 10^6$ is taken. Thus, this stiffness value can be used to treat the spring system as rigid. In Table 1, direct comparison can be made with the results of Laura *et al.* [8] for $(n, s) = (0, 0)$ and $K_w a^3/D = 10^1, 10^2$ and they are found to agree. The Rayleigh-Ritz method was used in [8].

Consider next the more general problem of a free circular plate elastically constrained by uniform translational and rotational springs along parts of the edge. The stiffness of each spring may vary independently from the others. For instance, when a plate is constrained along two opposite circular parts ($-\alpha < \theta < \alpha, \pi - \alpha < \theta < \pi + \alpha$) of the edge, the spring system along the entire boundary is expanded into a Fourier cosine series with coefficients

$$\begin{aligned}\bar{K}_m &= \frac{1}{\pi} \int_0^{2\pi} (K_w a^3/D) \cos m\theta \, d\theta \\ &= \frac{2}{m\pi} (\bar{K}_w^{(1)} + \bar{K}_w^{(2)} \cos m\pi) \sin m\alpha \quad (m = 1, 2, \dots)\end{aligned}\quad (18a)$$

for the translational spring, and

$$\bar{L}_m = \frac{2}{m\pi} (\bar{K}_\psi^{(1)} + \bar{K}_\psi^{(2)} \cos m\pi) \sin m\alpha \quad (m = 1, 2, \dots)\quad (18b)$$

for the rotational spring in the same fashion, with $\bar{K}_w^{(i)} = K_w^{(i)} a^3/D$, $\bar{K}_\psi^{(i)} = K_\psi^{(i)} a^3/D$.

To investigate the rate of convergence the method on this problem, a test case was chosen wherein the plate is effectively clamped ($\bar{K}_w^{(1)} = \bar{K}_\psi^{(1)} = 10^6$) along one-quarter of its edge and free along the remaining three-quarters. This is an especially severe case because of the presence of both moment and shear singularities at the points of discontinuity. Furthermore, the strengths of these singularities are more pronounced than, say, if half the edge were clamped. The results of the convergence study are seen in Table 2, wherein the size of the determinant required to obtain three significant figure accuracy for the first six modes is clearly seen. It is noted that the rate of convergence is different for the different modes. Based upon this study, subsequent calculations throughout the paper are carried out using 60th order determinants. Poisson's ratio of 0.33 is also used throughout.

Applying the method to the more general case, Fig. 2 shows the lowest six frequency

Table 1. Frequency parameters of a circular plate uniformly constrained by a translational spring along its edge ($\nu = 0.33$)

Mode Sequence	(n, s)	$K_w a^3/D$							
		0 (Free)	10^{-1}	10^0	10^1	10^2	10^4	10^6	∞ (s.s.)
1	(0,0)	0	0.668	1.172	1.861	2.183	2.231	2.231	2.231
2	(1,0)	0	0.795	1.410	2.440	3.479	3.731	3.733	3.733
3	(2,0)	2.294	2.305	2.398	2.983	4.370	5.057	5.064	5.064
4	(0,1)	3.012	3.016	3.052	3.390	4.701	5.447	5.455	5.455
5	(3,0)	3.499	3.503	3.536	3.822	5.068	6.308	6.324	6.324
6	(1,1)	4.529	4.530	4.541	4.648	5.567	6.949	6.965	6.965

Table 2. Convergence study of frequency parameters of a free circular plate constrained along a quarter part of the edge ($\nu = 0.33$, $\bar{K}_w^{(1)} = K_w^{(1)} = 10^6$)

Matrix Size	Mode					
	1	2-A	2-S	3-S	3-A	4
20x20	1.18	1.87	2.67	3.10	3.47	4.28
30x30	1.14	1.82	2.61	3.08	3.39	4.18
40x40	1.12	1.80	2.59	3.07	3.37	4.14
50x50	1.11	1.79	2.57	3.07	3.35	4.12
60x60	1.10	1.78	2.56	--	3.34	4.11
70x70	1.10	1.78	2.55		3.34	4.10
80x80	--	--	2.55		--	4.09
90x90			--			4.09

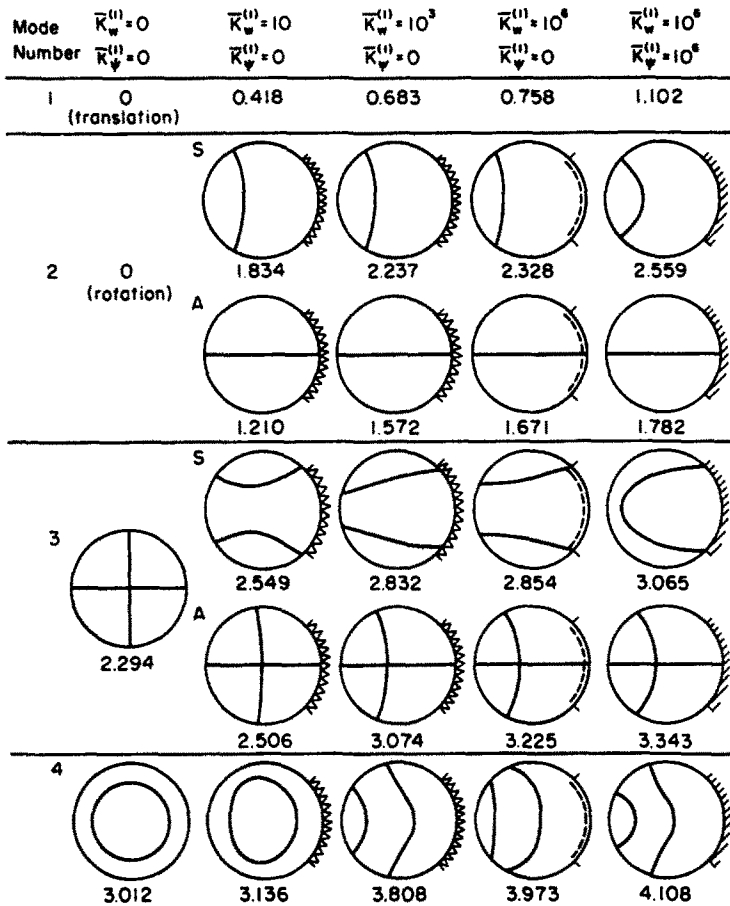


Fig. 2. Frequency parameters and nodal patterns of a circular plate constrained by partial translational and rotational springs ($\nu = 0.33$, $\alpha/\pi = 1/4$).

parameters and nodal patterns of circular plates elastically constrained by translational and rotational springs along a quarter part of the edge. The solid lines shown inside the circular boundary denote nodal lines; i.e. lines of zero deflection. The fundamental modes have no internal nodal lines. In this figure, moving from left to right, the stiffness of the translational spring is gradually increased, starting from a completely free plate and going to a plate simply supported along a quarter of its boundary. Then sufficient rotational rigidity is added to make the boundary segment effectively clamped. The generation of two sets of modes, symmetric and

anti-symmetric, from the degenerate modes of a completely free circular plate having one and two nodal diameters, is clearly seen.

A more comprehensive study of the variations of the frequency parameters with increasing spring stiffness is shown in Fig. 3, where the first ten modes are presented. Solid lines denote symmetric modes and broken lines anti-symmetric modes. In Fig. 3(a) only the translational spring stiffness varies, whereas in Fig. 3(b) only the rotational spring stiffness varies. It is observed from Figs. 3(a) and (b) that considerable increases of frequency parameters take place between nondimensional rigidities 10^0 and 10^3 for both types of springs.

Figure 4 shows variations of frequency parameters with the change of angle for a plate constrained along one part of the edge. Since the stiffnesses are taken as $\bar{K}_w^{(1)} = 10^6$ and

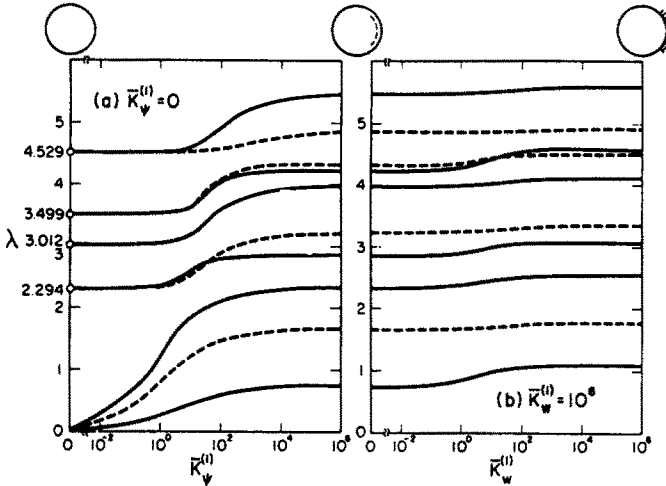


Fig. 3. Variation of frequency parameters of a circular plate constrained by partial translational and rotational springs ($\nu = 0.33$, $a/\pi = 1/4$). (a) $\bar{K}_\psi^{(1)} = 0$, (b) $\bar{K}_w^{(1)} = 10^6$.

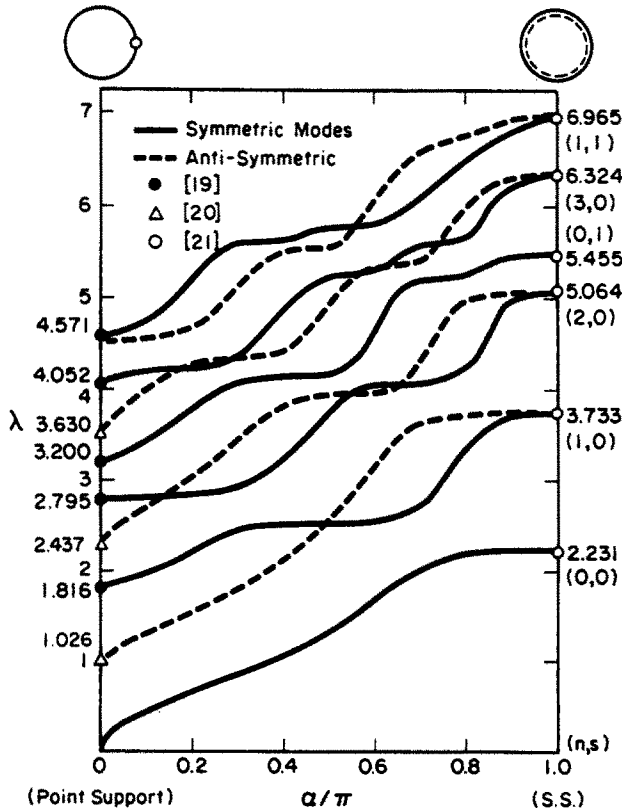


Fig. 4. Variation of frequency parameters with the angle of constraint for a simply-supported, free plate ($\nu = 0.33$, $\bar{K}_w^{(1)} = 10^6$).

$\bar{K}_\psi^{(1)} = 0$, the constrained part of the plate can be considered effectively simply supported. Irie and Yamada [19] have obtained frequencies of a free circular plate supported at a point, and the present values for symmetric modes are in good agreement with their values in the vicinity of $\alpha = 0$. The differences of these values of λ are less than 0.1%, when $\alpha = 0.01$ is taken. For anti-symmetric modes, a finite angle 2α of simple support, no matter how small, has a clamping effect at $\theta = 0$ in the circumferential direction. Consequently, the frequency parameters approach those presented in the figure, which were obtained by Yamada [20] for a plate clamped in both directions at a point. On the other hand, the plate becomes simply supported uniformly all around as α approaches π . The limiting values of λ for $\alpha = 0$ [19, 20] and π [21] are presented in the figure. The number of nodal diameters (n) and interior nodal circles (s) for these limiting cases are also given.

In Fig. 5, stiffnesses are taken as $\bar{K}_w^{(1)} = \bar{K}_\psi^{(1)} = 10^6$ and the constrained part is therefore essentially clamped. The frequency parameters vary between those of a point clamped ($\alpha = 0$) and completely clamped ($\alpha = \pi$) circular plate. As α approaches zero, the present values approach those of Yamada [20] for a point clamped plate whose rotation is rigidly constrained at the point in both radial and circumferential directions. It is observed that frequency variations of the corresponding modes in both Figs. 4 and 5 show similar trends, with the curves of different modes of the same symmetric class approaching each other and veering away.

Finally, the results of Fig. 5 can be compared with those of Torvik [16], who used this problem to demonstrate the application of a variational principle. In [16] experimental results for the problem, as well as ones obtained from a finite difference model (using approx. 2000 degrees of freedom) of the plate, are also given, and those of Fig. 5 are found to be quite accurate.

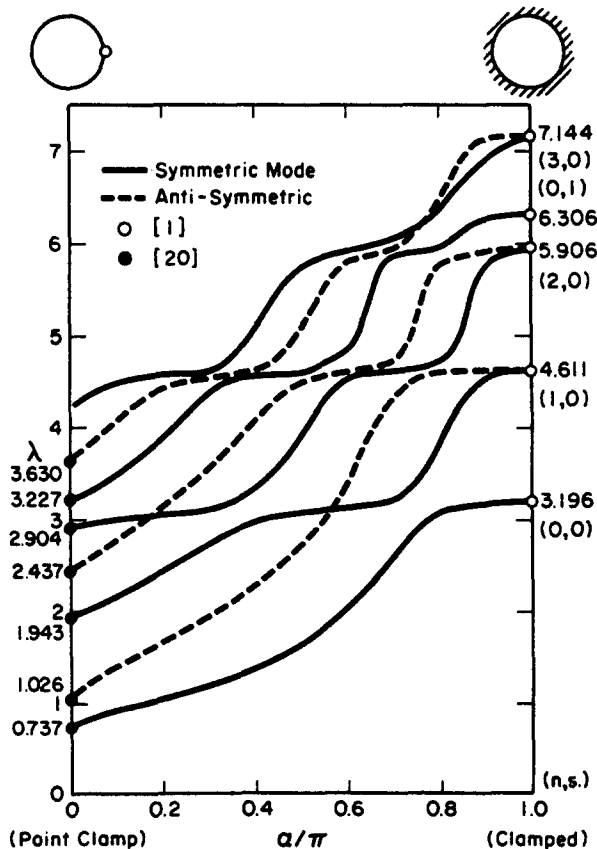


Fig. 5. Variation of frequency parameters with the angle of constraint for a clamped, free plate ($\nu = 0.33$, $\bar{K}_w^{(1)} = \bar{K}_\psi^{(1)} = 10^6$).

4. CONCLUDING REMARKS

In the present work, a straightforward method was presented to solve the classical plate equation subjected to general, nonuniform boundary conditions; i.e. mixed boundary conditions involving elastic constraints. The series-type method employed is quite suitable for computer programming, depending only upon the existence of appropriate Bessel function subroutines. The frequencies can be determined, as in other series-type methods, to the desired accuracy by using larger order determinants. A further extension of the method is possible to other plates having mixed boundary conditions, such as annular plates which involve Bessel functions of the second kind in the analysis. It will also be applicable to sectorial and annular sectorial plates having two straight simply supported edges if Bessel function subroutines are available for non-integer orders.

Acknowledgements—Most of the numerical calculations were carried out at Hokkaido University Computing Center and the authors gratefully acknowledge Professor T. Irie of Hokkaido University for his support of this research.

REFERENCES

1. A. W. Leissa, *Vibration of plates*. U.S. Government Printing Office, NASA SP-160 (1969).
2. A. W. Leissa, Recent research in plate vibrations. *Shock and Vib. Dig.* Part 1, 9, 13 (1977), Part 2, 10, 21 (1978).
3. A. W. Leissa, The free vibration of rectangular plates. *J. Sound Vib.* 31, 257 (1973).
4. C. L. Kantham, Bending and vibration of elastically restrained circular plates. *J. Franklin Inst.* 265, 483 (1958).
5. K. Singa Rao and C. L. Amba-Rao, Lateral vibration and stability relationship of elastically restrained circular plates. *AIAA J.* 10, 1689 (1972).
6. P. A. A. Laura, J. C. Paloto and R. D. Santos, A note on the vibration and stability of a circular plate elastically restrained against rotation. *J. Sound Vib.* 41, 177 (1975).
7. P. A. A. Laura and R. Gelos, Fundamental frequency of vibration of a circular plate elastically restrained against rotation and carrying a concentrated mass. *J. Sound Vib.* 45, 298 (1976).
8. P. A. A. Laura, L. E. Luisoni and J. J. Lopez, A note on the free and forced vibrations of circular plates: the effect of support flexibility. *J. Sound Vib.* 47, 287 (1976).
9. W. Nowacki and Z. Olesiak, Vibration, buckling and bending of a circular plate clamped along part of its periphery and simply supported on the remaining part. *Bull. Acad. Pol. Sci.* 4, 247 (1956).
10. W. Nowacki and Z. Olesiak, The problem of a circular plate partially clamped and partially simply supported along the periphery (in Polish). *Arch. Mech. Stos.* 8, 233 (1956).
11. C. C. Bartlett, The vibration and buckling of a circular plate clamped on part of its boundary and simply supported on the remainder. *Quart. J. Mech. Appl. Math.* 16, 431 (1963).
12. B. Noble, The vibration and buckling of a circular plate clamped on part of its boundary and simply supported on the remainder. *Developments in Mechanics* 3, 141 (1965).
13. J. Vivoli and P. Fillippi, Eigenfrequencies of thin plates and layer potentials. *J. Acous. Soc. Am.* 55, 562 (1974).
14. F. G. Hemming, Investigation of natural frequencies of circular plates with mixed boundary conditions. Air Force Inst. Tech., School of Engng Rep. No. GAE/MC/75-11 (1975).
15. Y. Hirano and K. Okazaki, Vibration of a circular plate having partly clamped or partly simply supported boundary. *Bull. JSME* 19, 610 (1976).
16. P. Torvik, A variational approach to the dynamics of structures having mixed or discontinuous boundary conditions (to be published).
17. Y. Narita and A. W. Leissa, Transverse vibration of simply supported circular plates having partial elastic constraints. *J. Sound Vib.* 70, 103 (1980).
18. A. W. Leissa, P. A. A. Laura and R. H. Gutierrez, Transverse vibrations of circular plates having non-uniform edge constraint. *J. Acous. Soc. Am.* 66, 180 (1979).
19. T. Irie and G. Yamada, Free vibration of circular plate elastically supported at some points. *Bull. JSME* 21, 1602 (1978).
20. G. Yamada, Unpublished note.
21. A. W. Leissa and Y. Narita, Natural frequencies of simply supported circular plates. *J. Sound Vib.* 70, 221 (1980).